

## SOLVENT EFFECT ON HYPER-RAYLEIGH SCATTERING (HRS) FIRST HYPERPOLARIZABILITY OF SUBSTITUTED POLYENE: PART (I)

N. S. Labidi

Institut des Sciences et de la Technologie, Département des Sciences de la Matière, Centre  
Universitaire de Tamanrasset.11000 Tamanrasset, Algérie

Received: 07 October 2020 / Accepted: 24 July 2021 / Published online: 01 September 2021

### ABSTRACT

The first hyperpolarizabilities  $\beta_{\text{HRS}}$  of substituted hexatriene molecules have been carried out to assess the effects of the bridge length, of the frequency dispersion as well as the solvent polarity. These calculations confirm the particular behaviour of the first hyperpolarizability  $\beta_{\text{HRS}}$ , depolarization ratio and the anisotropy factor as a function of the incident light frequency and solvent polarity. The impact of the solvent and expanding the  $\pi$ -conjugated limit to improve the  $\beta_{\text{HRS}}$ . Finally, the interplay between  $\beta_{\text{HRS}}$  and  $\beta_{\parallel}$ ,  $\beta_{\text{vec}}$ ,  $d_{\text{N...N}}$ ,  $E_{\text{gap}}$  and the Kirkwood–Onsager factor  $[(\epsilon-1)/(2\epsilon + 1)]$  was established.

**Keywords:** First hyperpolarizability; Hyper-Rayleigh scattering (HRS); push-pull; solvent

Author Correspondence, e-mail: [labidi19722004@yahoo.fr](mailto:labidi19722004@yahoo.fr)

doi: <http://dx.doi.org/10.4314/jfas.v13i3.2>

### 1. INTRODUCTION

Many research efforts have been devoted to nonlinear effects in organic compounds essentially due to their significant potential in photonics and optoelectronics applications, as well as the appropriate development of computational capabilities [1–3]. Conjugated molecules, characterized by a polarizable  $\pi$ -electron bridge that separates an electron donor



group (D) from an electron acceptor group (A), were extensively investigated as potential efficient nonlinear optics (NLO) compounds. Push- $\pi$ -pull molecules are interesting in this regard because of their intrinsic properties at the microscopic scale, they typically possess a large dipole moment that induce asymmetric polarization between opposite end groups playing crucial roles in the intramolecular charge transfer (ICT) associated with an extremely high molecular non linear optical response [4-7]. The most used way of varying NLO properties is by chemical way which is not a simple task. However, before any experiment addressing properties of molecules presenting nonlinear optical (NLO) response, it is crucial to employ methods of molecular modeling to predict the desired properties by finding appropriate interplay between many molecular parameters (length, shape of the bridges, strengths and positions of the electron donor and acceptor groups) [8-12]. The use of quantum chemical calculations to evaluate the Hyper-Rayleigh scattering (HRS) hyperpolarizability in agreement with experimental results is a big deal for computational chemists.

This study deals with the solvent effects on the NLO responses in a series of push-pull polyenes [D- $\pi$ -NO<sub>2</sub>] that have been proposed in view of achieving large second-order NLO responses. Here, we present the results, starting with an investigation of the bridge lengths effects, the frequency dispersion for the selected system as well as the effects of the solvent polarity on the first hyperpolarizability ( $\beta_{\text{HRS}}$ ) responses, energy gap and bond length alternation (BLA). Finally, the relationships between the first hyperpolarizability ( $\beta_{\text{HRS}}$ ) and  $\beta_{//}$ ,  $\beta_{\text{vec}}$ , separation distance ( $d_{\text{N...N}}$ ), energy gap ( $E_{\text{gap}}$ ) and the Kirkwood–Onsager factor  $[(\epsilon-1)/(2\epsilon + 1)]$  are established.

## 2. METHODOLOGY AND COMPUTATIONAL DETAILS

The molecular structures were optimized in a vacuum and in acetonitrile solvent at the density functional theory (DFT) level using the B3LYP exchange–correlation functional and the 6-311G\* basis set. To take into account the solvent effects the polarizable continuum model within the integral equation formalism (IEF-PCM) [13] was employed at 6-31+G\* and 6-311+G\* basis sets. The dynamic  $\beta_{\text{HRS}}(-2\omega;\omega,\omega)$  and static  $\beta_{\text{HRS}}(0;0,0)$  first

hyperpolarizabilities were evaluated with different schemes. Firstly, at the time-dependent Hartree–Fock (TDHF) and coupled perturbed Hartree–Fock (CPHF) [14, 15].

Champagne and co-workers [16-18] developed an effective method to evaluate the hyper-Rayleigh scattering (HRS) response  $\beta_{HRS}(-2\omega; \omega, \omega)$ , which is described as:

$$\beta_{HRS}(-2\omega; \omega, \omega) = \sqrt{(\langle \beta_{ZZZ}^2 \rangle + \langle \beta_{ZXX}^2 \rangle)} \dots \dots \dots (1)$$

$\langle \beta_{ZZZ}^2 \rangle$  and  $\langle \beta_{ZXX}^2 \rangle$  are the orientational averages of the molecular  $\beta$  tensor components.

In addition, the molecular geometric information is given by the depolarization ratio (DR), which is expressed by:

$$DR = \frac{\langle \beta_{ZZZ}^2 \rangle}{\langle \beta_{ZXX}^2 \rangle} \dots \dots \dots (2)$$

For an ideal D/A 1D system  $DR = 5$ , the amplitude of DR depends on the angle between the chromophores as well as on the strengths of the D/A groups) [17, 18].

On the other hand, the central quantity  $\beta_{//}(-2\omega; \omega, \omega)$  corresponds to the projection of the vector part of  $\beta$  on the dipole moment vector:

$$\beta_{//}(-2\omega; \omega, \omega) = \frac{3}{5} \sum_i \frac{\mu_i \beta_i}{\|\mu\|} \dots \dots \dots (3)$$

where  $\|\mu\|$  is the norm of the dipole moment and  $\mu_i$  and  $\beta_i$  are the components of the  $\mu$  and  $\beta$  vectors.

The relative contribution of the octupolar and dipolar components is given by the nonlinear anisotropy ratio:

$$\rho = \frac{|\beta_{J=3}|}{|\beta_{J=1}|} \dots \dots \dots (4)$$

Where  $(\beta_{J=1})$  and  $(\beta_{J=3})$  are the dipolar and octupolar contributions of the  $\beta$  response.

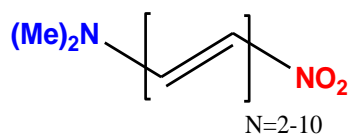
Then, the nonlinear anisotropy parameter  $\rho = |\beta_{J=3}|/|\beta_{J=1}|$  is employed to evaluate the ratio of the octupolar [ $\Phi_{\beta J=3} = \rho/(1 + \rho)$ ] and dipolar [ $\Phi_{\beta J=1} = 1/(1 + \rho)$ ] contribution to the hyperpolarizability tensor.

All reported  $\beta$  values are given in a.u. [1 a.u. of  $\beta = 3.6213 \times 10^{-42} \text{ m}^4 \text{ V}^{-1} = 3.2064 \times 10^{-53} \text{ C}^3 \text{ m}^3 \text{ J}^{-2} = 8.639 \times 10^{-33} \text{ esu}$ ] within the T convention. All calculations were performed using the Gaussian 09 program [19].

### 3. RESULTS AND DISCUSSION

#### 3.1. Effect of bridge length

In Fig. 1 and Table S1 (Supporting information), we present the dependence of the first hyperpolarizability  $\beta_{\text{HRS}}$  and depolarization ratio (DR) on  $d_{\text{N}\dots\text{N}}$  separation distance ( $\text{\AA}$ ) between  $\text{NO}_2/\text{N}(\text{Me})_2$  end groups for a series of all-trans  $\alpha,\omega$ -nitro,dimethylamino-polyene  $[\text{NO}_2-(\text{CH}=\text{CH})_N-\text{N}(\text{Me})_2]$  (Scheme 1), calculated at the HF/6-31+G\* basis set with and without taking into account the effects of the solvent (acetonitrile) using the IEFPCM scheme.



**Scheme1.** Structure of the all-trans  $\alpha,\omega$ -nitro,dimethylamino-polyene  $[\text{NO}_2-(\text{C}=\text{C})_N-\text{N}(\text{Me})_2]$

In general, the static and dynamic  $\beta_{\text{HRS}}$  has an uptrend with increasing the separation distance ( $d_{\text{N}\dots\text{N}}$ ) for all-trans  $\alpha,\omega$ -nitro,dimethylamino-polyene molecules. The dynamic ( $\lambda = 1064$  nm)  $\beta_{\text{HRS}}$  in acetonitrile increases even more rapidly than in vacuum with increasing the separation distance ( $d_{\text{N}\dots\text{N}}$ ) (see Scheme S1) between the two end groups  $\text{NO}_2/\text{N}(\text{Me})_2$ . The static first hyperpolarizability  $\beta_{\text{HRS}}$  in vacuum and in acetonitrile solvent appears to be linearly dependent on the  $\text{NO}_2/\text{N}(\text{Me})_2$   $d_{\text{N}\dots\text{N}}$  separation distance. However, the dynamic  $\beta_{\text{HRS}}$  grow exponentially with the substituted polyene length in Fig. 1a.

In order to clarify this increasing degree, the vacuum dynamic  $\beta_{\text{HRS}}$  ( $\lambda = 1064\text{nm}$ ) versus its static value in acetonitrile is plotted in Fig. 1b. As can be seen, a linear relationship is obtained with a slope of 3.77 and a correlation coefficient of unity  $R=1.00$ . The comparison reveals that the solvent effect considerably enhances the HRS first hyperpolarizability, the quantified solvent effect ratio ( $\beta_{\text{HRS}}^{\text{sol}}/\beta_{\text{HRS}}^{\text{vac}}$ ) range from 2 for a separation distance of  $d_{\text{N}\dots\text{N}} = 6.1\text{\AA}$  to 4 for  $d_{\text{N}\dots\text{N}} = 25.8\text{\AA}$ . In addition, since both dynamic and static depolarization ratio is about unity ( $\text{DR}^{\text{sol}}/\text{DR}^{\text{vac}} \sim 1.00$ ), one can say that the acetonitrile solvent has little effect on DR.

The results of HF calculations in gas phase and acetonitrile related to the level of theory using 6-31+G\* and 6-311+G\* bases show a slight difference, the quantified ratios for the dynamic ( $\lambda=1064\text{nm}$ ) hyperpolarizability i.e.: in acetonitrile the ratios  $\beta_{\text{HRS}}(6-31+G^*)/$

$\beta_{\text{HRS}}(6\text{-}311+\text{G}^*)$  range from 0.99 for  $d_{\text{N}\dots\text{N}} = 6.1\text{\AA}$  to 0.94 for  $d_{\text{N}\dots\text{N}} = 25.8\text{\AA}$  and in vacuum  $\beta_{\text{HRS}}(6\text{-}31+\text{G}^*)/\beta_{\text{HRS}}(6\text{-}311+\text{G}^*) = 1.00$  for  $d_{\text{N}\dots\text{N}} = 6.1\text{\AA}$  to 0.99 for  $d_{\text{N}\dots\text{N}} = 25.8\text{\AA}$ . Similar conclusions are drawn when employing the 6-31+G\* and 6-311+G\* basis sets.

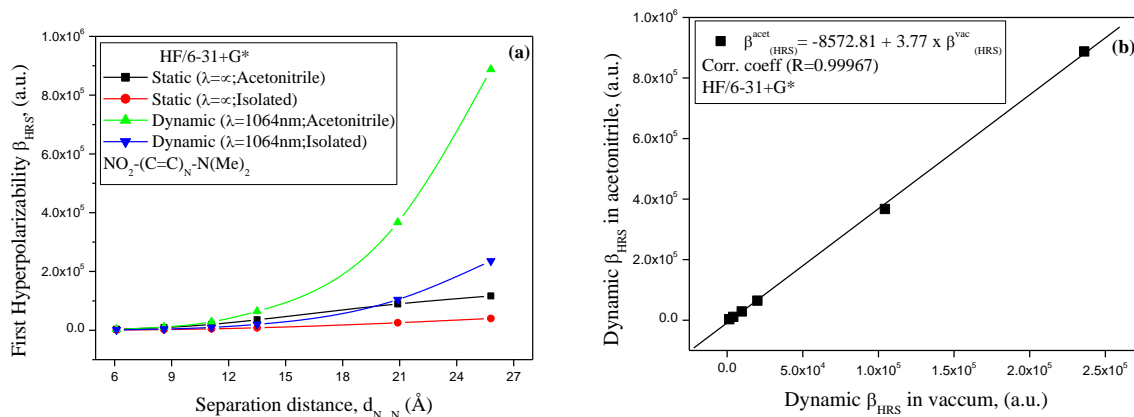


**Fig. 1.** Variation of first hyperpolarizability  $\beta_{\text{HRS}}$  with the  $\text{O}_2\text{N}/\text{N}(\text{Me})_2$  separation distance (a);  $\beta_{\text{HRS}}$  in acetonitrile versus its value in vacuum at  $\lambda = 1064\text{ nm}$  (b)

The dependence of the first hyperpolarizability  $\beta_{\text{HRS}}$  on the separation distance  $d_{\text{N}\dots\text{N}} = 6.1\text{\AA}$  to  $25.8\text{\AA}$  between the  $\text{O}_2\text{N}/\text{N}(\text{Me})_2$  end groups in all-trans  $\alpha,\omega$ -nitro,dimethylamino-polyene considering the isolated and the solvated (acetonitrile) molecules at the HF/6-31+G\* level of theory, reveal a linear dependence for the static  $\beta_{\text{HRS}}^\infty$  (Fig.2a), while the dynamic first hyperpolarizability  $\beta_{\text{HRS}}^{1064}$  appears to grow exponentially (Fig.2b). The following relations have been obtained:

For the static ( $\lambda = \infty$ )

$$\beta_{\text{HRS}} = -41731.31 + 6104.91 \times d_{\text{N}\dots\text{N}} \quad (\text{Acetonitrile, } R=0.99)$$

$$\beta_{\text{HRS}} = -15652.54 + 2048.01 \times d_{\text{N}\dots\text{N}} \quad (\text{Isolated, } R=0.98)$$

For the dynamic ( $\lambda = 1064\text{nm}$ )

$$\beta_{\text{HRS}} = 1031 \exp(0.274 \times d_{\text{N}\dots\text{N}}) \quad (\text{Acetonitrile, } R=0.99)$$

$$\beta_{\text{HRS}} = 463.3 \exp(0.252 \times d_{\text{N}\dots\text{N}}) \quad (\text{Isolated, } R=0.99)$$

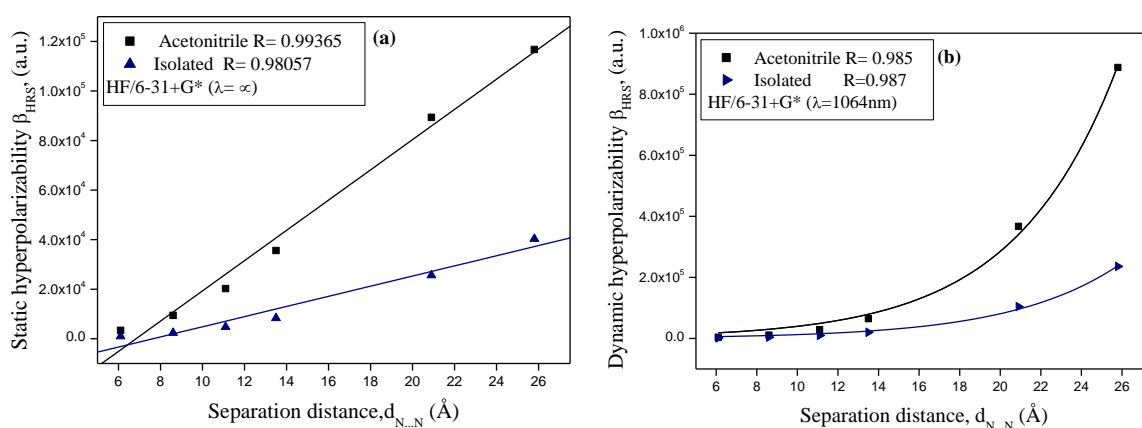
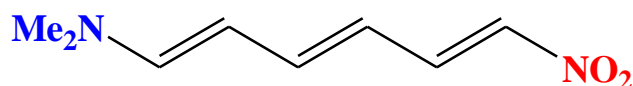


**Fig. 2.** Dependence of the static (a) and dynamic (b) first hyperpolarizability as function of  $O_2N/N(Me)_2$  separation distance in vacuum and acetonitrile (solvent)

### 3.2 Frequency dispersion effects

The dynamic perturbations were added in order to explore the effect of frequency dispersion. For comparison, fundamental optical wavelengths range with  $\lambda = \infty - 1823$  nm (Corresponding to a frequency range  $\omega = 0.0 - 0.095$  a.u) were used to reveal the dispersion correction contribution to the NLO response in all-trans  $\alpha,\omega$ -nitro,dimethylamino-hexatriene (Scheme 2).



**Scheme 2.** Structure of the all-trans  $\alpha,\omega$ -nitro,dimethylamino-Hexatriene

Fig. 3 and Table S2 (Supporting Information) describe the variations of first hyperpolarizability ( $\beta_{HRS}$ ) of all-trans  $\alpha,\omega$ -nitro, dimethylamino-hexatriene as a function of the excitation frequency in parallel with the variation of the depolarization ratio (DR). As shown in Table S2 (Supporting Information), the comparison of the TDHF/6-311+G\* dynamic  $\beta_{HRS}$  values obtained in vacuum and in acetonitrile reveals that the solvent effect significantly enhances the HRS hyperpolarizabilities of the substituted hexatriene molecule, the dynamic  $\beta_{HRS}$  in acetonitrile increases even more rapidly than in vacuum with increasing the optical wavelengths range ( $\lambda = \infty - 1823$ nm) and the solvent dependent first hyperpolarizability for applied frequencies increases by 15–98%. The frequency dependence hyperpolarizability  $\beta_{HRS}$

in the vacuum and acetonitrile tend to follow each other as illustrated by the quantified solvent effect factor  $\beta_{\text{HRS}}^{(\text{Acetonitrile})} / \beta_{\text{HRS}}^{(\text{Isolated})}$  ranging from 2 to 4.

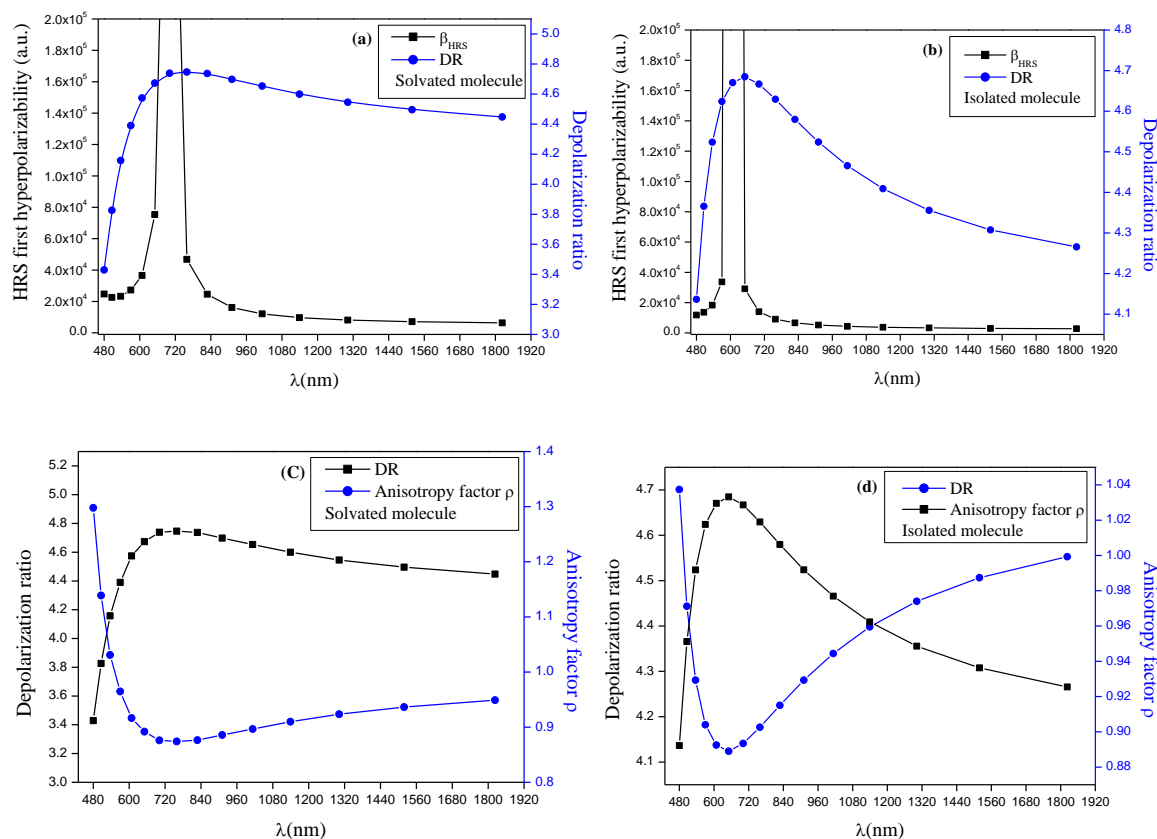


**Fig. 3.** Evolution of the first hyperpolarizability  $\beta_{\text{HRS}}$ , depolarization ratio and anisotropy factor with the incident light frequency for solvated (a and c) and isolated (b and d)  $\alpha,\omega$ -nitro, dimethylamino-Hexatriene determined at the TDHF/6-311+G\* basis set

In Fig. 3a, the  $\beta_{\text{HRS}}$  versus  $\lambda(\text{nm})$  curve for solvated (acetonitrile) molecule presents a curve, whose peak at  $\lambda = 701 \text{ nm}$  is related to the predicted resonance region  $\omega = 0.06\text{--}0.07$  (a.u.). In the same range of frequency, the depolarization ratio displays an accelerating trend and changes slightly. Indeed, DR amounts to roughly 3.43 in the low frequency region, increases with the frequency up to a value close to 4.74 for  $\lambda = 701 \text{ nm}$ . These variations originate from the types of tensor components, which dominate the first hyperpolarizability  $\beta_{\text{HRS}}$  response. Indeed, the macroscopic averages diagonal  $\langle \beta_{zzz}^2 \rangle$  component dominates the response at small frequencies up to about  $\omega = 0.065$  (a.u.), then the off-diagonal  $\langle \beta_{zxx}^2 \rangle$  components become dominant. Dissimilar variations of  $\beta_{\text{HRS}}$  are observed for the isolated

molecule as shown in Fig. 3b, the HRS first hyperpolarizability presents a peak at  $\lambda = 608$  nm whereas the depolarization ratio DR changes considerably in the predicted resonance region between  $\omega = 0.07-0.08$  (a.u.) to achieve a maximum value of 4.68 at  $\lambda = 651$  nm, then strongly decreases between  $\lambda = 701$  nm and 1823 nm to attain the smallest value close 4.27 in this range of frequency. In addition, since the frequency dependant  $DR^{(\text{Acetonitrile})}/DR^{(\text{Isolated})}$  ratio ranges from 0.83 to 1.04 and  $\rho^{(\text{Acetonitrile})}/\rho^{(\text{Isolated})}$  ranges from 0.95 to 1.25, the solvent acetonitrile has little effect on depolarization ratio (DR) and anisotropy factor ( $\rho$ ).

To further explore the evolution of depolarization ratio (DR) and the anisotropy factor ( $\rho$ ) with respect to the variation of frequency dispersion, Table S2 (Supporting Information) describes the variations of applied frequency excitation as a function of the anisotropy factor ( $\rho$ ) in parallel with the variations of the depolarization ratio (DR). For the solvated (acetonitrile) molecule as depicted by Fig. 3c, an inverse relationship was found between DR and the anisotropy factor ( $\rho$ ), the DR value decreases along with increasing  $\rho$  covering the range of the incident light frequency from  $\omega = 0.025$  to 0.095 (a.u.). In this frequency region, the DR value increases along with decreasing  $\rho$  from 3.43 to 4.45, covering the wide anisotropy factor range from 1.30 to 0.95. Moreover, the curve displays extremum values around 759 nm within a maximum of DR close to 4.75 corresponds with him a minimum value of the anisotropy factor  $\rho = 0.87$ . However, in the frequency region between  $\lambda = 828$  nm to 1823 nm we perceive the convergence of the curves and therefore the parameters (DR and  $\rho$ ) with a reduction effect between them. On the other hand, the situation is similar for the isolated molecule when considering a frequency dispersion variation from  $\omega = 0.095$  (a.u.) to 0.04 (a.u.) as exposed in Fig. 3d, the DR initially increases along with decreasing  $\rho$  from 4.14 to 4.41, covering the wide anisotropy factor range from 1.04 to 0.96. Then, it displays the highest value close to 4.68 covering a value of anisotropy factor  $\rho$  of 0.89. However, in the frequency region  $0.04$  (a.u.)  $\leq \omega \leq 0.025$  (a.u.), an overturn behaviour is observed producing a considerable increase in anisotropy factor ( $\rho$ ) to the highest value of 1.00 versus a rough decrease in DR to attain the least value close to 4.27.



### 3.3. Solvent polarity effects

#### 3.3.1. Solvent polarity effect on first hyperpolarizability

To model the effect of solvent polarity, the static and dynamic  $\beta_{\text{vec}}$ ,  $\beta_{//}$ ,  $\beta_{\text{HRS}}$  and depolarization ratio (DR) of all-trans  $\alpha,\omega$ -nitro,dimethylamino-hexatriene in a variety of solvents ranging dielectric constants from  $\epsilon = 2.27$  (benzene) to  $\epsilon = 46.83$  (dimethylsulfoxide) [20-21] are calculated at the TDHF level of approximation with 6-311+G\* basis set and presented in Table S3(Supporting Information).

Fig. 4a and Fig.4b show a different affinity for the static and the dynamic hyperpolarizabilities. i) the solvent polarity alter the hyperpolarizabilities behaviour, numerically the dynamic ( $\lambda = 1064\text{nm}$ )  $\beta_{//}$ ,  $\beta_{\text{vec}}$  and  $\beta_{\text{HRS}}$  are more than those calculated at ( $\lambda = \infty$ ) with increasing the dielectric constant ( $\epsilon$ ) of the medium, for both static and dynamic hyperpolarizability it can be verified that  $\beta_{\text{vec}} > \beta_{//} > \beta_{\text{HRS}}$ .

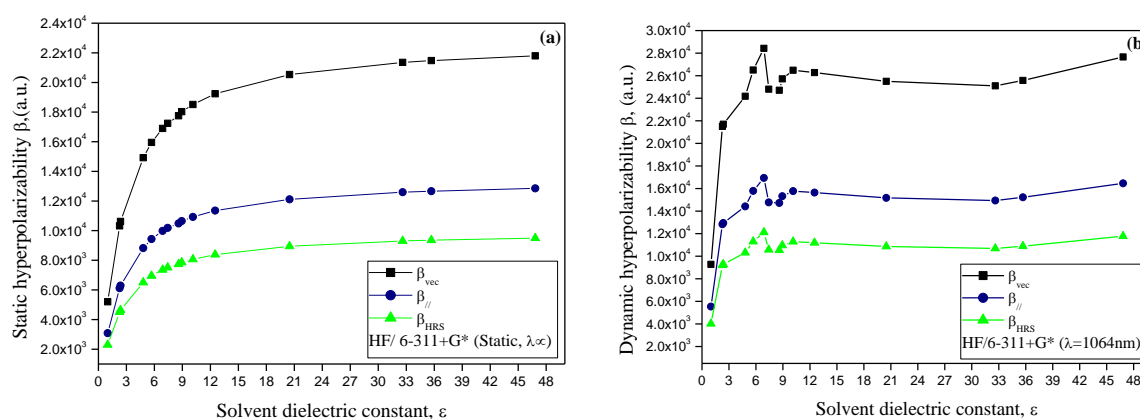


**Fig. 4.** Solvent polarity effects on calculated static (a) and dynamic (b):  $\beta_{\text{vec}}$ ,  $\beta_{//}$ ,  $\beta_{\text{HRS}}$  for all-trans  $\alpha,\omega$ -nitro,dimethylamino-Hexatriene at the HF/ 6-311+G\* level of approximation

As noted in Table S3 (Supporting Information) for solvent dielectric constant ranging from  $\epsilon=1$  to 46.86, the values of dynamic (1064nm)  $\beta_{\text{vec}}$  go from 9279.6 (a.u.) to 27659.7 (a.u.) ,  $\beta_{//}$  go from 5535.7 (a.u.) to 16461.2 (a.u.) and  $\beta_{\text{HRS}}$  go from 4015.5(a.u.) to 11775.0(a.u.). The calculated hyperpolarizabilities  $\beta_{//}$ ,  $\beta_{\text{vec}}$  and  $\beta_{\text{HRS}}$  increase about 2-4 times from gas phase ( $\epsilon = 1$ ) to DMSO ( $\epsilon=46.83$ ). The ratios of dynamic and static quantities ( $\beta_{//}$ ,  $\beta_{\text{vec}}$  and  $\beta_{\text{HRS}}$  (1064 nm))/ ( $\beta_{//}$ ,  $\beta_{\text{vec}}$  and  $\beta_{\text{HRS}}$  ( $\lambda=\infty$ )) are about 2 times respectively. At  $\lambda=1064\text{nm}$  hyperpolarizabilities

present increased oscillations from benzene ( $\epsilon = 2.27$ ) to 1-Hexanol ( $\epsilon = 12.51$ ) and exhibits a peak for aniline ( $\epsilon = 6.89$ ) and a rather poor agreement with respect to the increasing ( $\epsilon$ ) value, in this region the ratios between the calculated dynamic and static values are  $\beta_{\text{HRS}}(1064 \text{ nm}) / \beta_{\text{HRS}}(\lambda=\infty) = 1.34\text{--}2.00$ ,  $\beta_{//}(1064 \text{ nm}) / \beta_{//}(\lambda=\infty) = 1.38\text{--}2.10$  and  $\beta_{\text{vec}}(1064 \text{ nm}) / \beta_{\text{vec}}(\lambda=\infty) = 1.37\text{--}2.08$ ; ii) the static ( $\lambda=\infty$ ) first hyperpolarizabilities  $\beta_{//}$ ,  $\beta_{\text{vec}}$  and  $\beta_{\text{HRS}}$  initially increase monotonically with an increase in the dielectric constant of the solvent ( $\epsilon = 1$  to 13) but attain an almost constant value for solvents of higher dielectric constants ( $\epsilon$ ) and nearly saturated at acetone ( $\epsilon = 20.49$ ), consequently hyperpolarizabilities are less influenced by more polar solvents; iii) an increase of the DR values with the increase in the solvent dielectric constant ( $\epsilon$ ), the depolarization ratio (DR) increases noticeably in the region of  $\epsilon = 1\text{--}13$  and gradually comes to saturation in the region of  $\epsilon = 13\text{--}47$ . In addition, for the dynamic ( $\lambda = 1064\text{nm}$ ) values the solvent effect factor  $\text{DR}^{\text{sol}}/\text{DR}^{\text{vac}}$  ranges from 1.03 for benzene and toluene to 1.05 for acetone, methanol, acetonitrile and DMSO. The solvent polarity has little effect on DR.

The evaluate the solvent polarity effect between the macroscopic averages diagonal  $\langle \beta^2_{zzz} \rangle$  and off-diagonal  $\langle \beta^2_{zxx} \rangle$  components of the  $\beta_{\text{HRS}}$  tensor, we plot in Fig. 5 the relationship between the ratio  $\langle \beta^2_{zxx} \rangle / \langle \beta^2_{zzz} \rangle$  of all-trans  $\alpha,\omega$ -nitro, dimethylamino-hexatriene with increasing in the solvent polarity. Fig. 5 and Table S4 (Supporting Information) show, that with increasing the dielectric constant of the solvent the static and dynamic ratios  $\langle \beta^2_{zxx} \rangle / \langle \beta^2_{zzz} \rangle$  decreases from 0.241 to 0.233 and from 0.226 to 0.216 respectively. Also, the relationship between the static and dynamic ratios  $\langle \beta^2_{zxx} \rangle$  and  $\langle \beta^2_{zzz} \rangle$  show an excellent linear dependence of  $\langle \beta^2_{zxx} \rangle$  on  $\langle \beta^2_{zzz} \rangle$  with increment in solvent polarity. The correlation coefficient is close to  $R = 1.00$  for the static and dynamic cases respectively, such linear correlations indicate that the rate of increase of  $\langle \beta^2_{zxx} \rangle$  due to solvent polarity is equal to that of  $\langle \beta^2_{zzz} \rangle$ . The result suggests that the off-diagonal component  $\langle \beta^2_{zxx} \rangle$  and the diagonal component  $\langle \beta^2_{zzz} \rangle$  have comparable solvent influence characteristic inducing a negligible solvent effect on the depolarization ratio (DR).

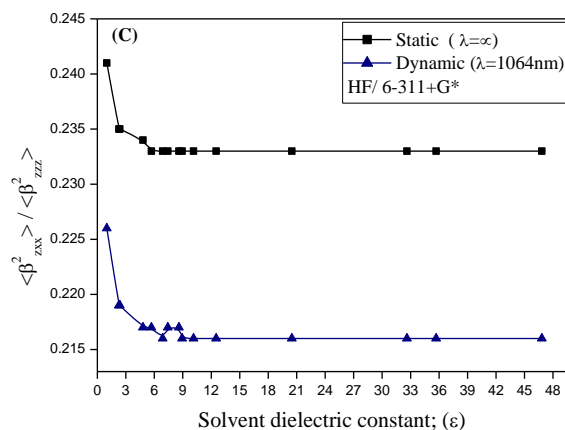


**Fig. 5.** Static and dynamic linear plot of the off-diagonal/ diagonal components  $\langle \beta_{zzz}^2 \rangle / \langle \beta_{xxx}^2 \rangle$  ratios in several solvents

To describe the contribution of electrostatic interactions of the solvent polarity, we plot the linear relationship between  $\beta_{\text{vec}}$ ,  $\beta_{//}$  and  $\beta_{\text{HRS}}$  values of all-trans  $\alpha,\omega$ -nitro, dimethylamino-hexatriene in various solvents versus the Kirkwood–Onsager dielectric factor  $D = (\epsilon - 1)/(2\epsilon + 1)$  [21]. The results in Fig. 6 and Table S4 (Supporting Information) show the connection between the static ( $\lambda = \infty$ ) and dynamic (1064nm) first hyperpolarizabilities values  $\beta_{\text{vec}}$ ,  $\beta_{//}$ ,  $\beta_{\text{HRS}}$  and the solvents dielectric factor (D).

As shown in Fig. 6a, an excellent agreement between static ( $\lambda = \infty$ ) first hyperpolarizabilities  $\beta_{\text{vec}}$ ,  $\beta_{//}$  and  $\beta_{\text{HRS}}$  and the dielectric scale  $(\epsilon - 1)/(2\epsilon + 1)$  ranging from zero to 0.5. The fitting results show a good correlation coefficient  $R = 0.99$ , respectively. In addition, the linear plot confirms that the dielectric factor works very well for all solvents series from nonpolar benzene ( $\mu = 0\text{D}$ ) to the polar aprotic media dimethylsulfoxide (DMSO) ( $\mu = 3.96\text{D}$ ). Whereas, the results for the dynamic (1064nm) dependence in Fig. 6b, shows rather poor agreement between  $\beta_{\text{vec}}$ ,  $\beta_{//}$ ,  $\beta_{\text{HRS}}$  and D (correlation coefficient  $R \approx 0.75$ ), with an apparent curvature of plot derives from the deviation of the data point of chlorobenzene, 1-chloropropane, aniline, and methanol. The slopes, intercepts and correlation coefficients of the least-squares straight-lines fit for static and dynamic  $\beta_{\text{vec}}$ ,  $\beta_{//}$  and  $\beta_{\text{HRS}}$  versus the Kirkwood–Onsager factor  $[(\epsilon - 1)/(2\epsilon + 1)]$  are given below:

For static ( $\lambda = \infty$ )

$$\beta_{\text{HRS}} = -261.15 + 19583.60 \times [(\epsilon - 1)/(2\epsilon + 1)] \quad (R = 0.99)$$

$$\beta_{vec} = -636.14 + 45036.60 \times [(\epsilon-1)/(2\epsilon+1)] \quad (R=0.99)$$

$$\beta_{//} = -315.22 + 26441.66 \times [(\epsilon-1)/(2\epsilon+1)] \quad (R=0.99)$$

For dynamic ( $\lambda=1064\text{nm}$ )

$$\beta_{HRS} = 7720.62 + 7621.91 \times [(\epsilon-1)/(2\epsilon+1)] \quad (R=0.75)$$

$$\beta_{vec} = 17916.83 + 18348.40 \times [(\epsilon-1)/(2\epsilon+1)] \quad (R=0.76)$$

$$\beta_{//} = 10734.00 + 10775.62 \times [(\epsilon-1)/(2\epsilon+1)] \quad (R=0.75)$$

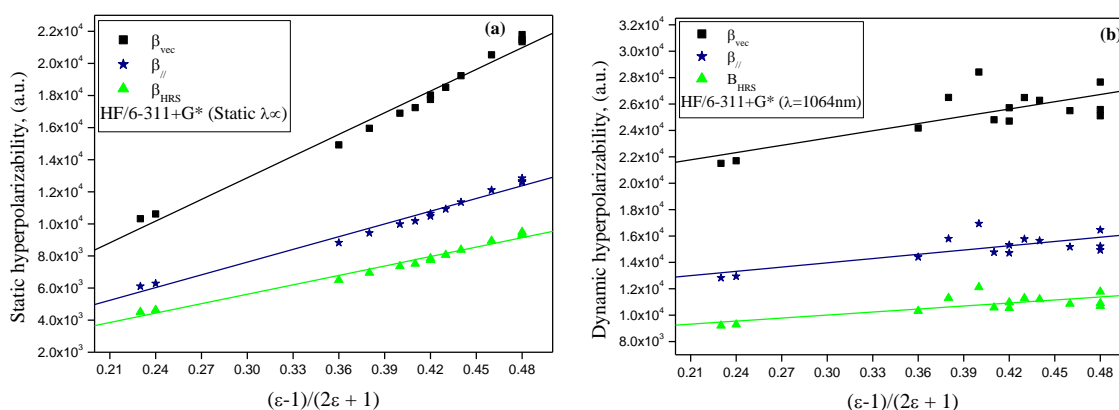


**Fig. 6.** Static (a) and dynamic (b) hyperpolarizabilities of all-trans  $\alpha,\omega$ -nitro, dimethylamino-Hexatriene as a function of the Kirkwood–Onsager factor  $(\epsilon-1)/(2\epsilon+1)$  of the solvent

### 3.3.2. Solvent polarity effect on energy gap ( $E_{gap}$ )

Fig. 7a and Fig.7b show the plot of energy gap  $E_{gap}$  and first hyperpolarizability ( $\beta_{HRS}$ ) as function of solvent dielectric constant ( $\epsilon$ ). As can be seen in Fig. 7a and Fig.7b, the energy gap ( $E_{gap}$ ) decrease with the increasing of the dielectric constant ( $\epsilon$ ) value of the solvent medium. The  $E_{gap}$  goes from 8.65 eV ( $\epsilon = 1.0$ ) to 8.23 eV ( $\epsilon = 46.83$ ) indicating that this property is appreciably affected by the solvent, as the solvent polarity increases  $E_{gap}$  decreases rapidly in the region of  $\epsilon=0-21$ , nearly saturating in acetone ( $\epsilon = 20.49$ ) and then gradually approaches a limiting value in the region of  $\epsilon=33-48$ . In addition, an inverse relationship was found between  $E_{gap}$  and first hyperpolarizability  $\beta_{HRS}$ . Strong polar solvent like DMSO, acetonitrile and methanol ( $\epsilon = 46.83, 35.69$  and  $32.61$ ) caused the  $E_{gap}$  to decrease,  $\alpha,\omega$ -nitro, dimethylamino-hexatriene molecule will exhibit the largest values of hyperpolarizability  $\beta_{HRS}$ .

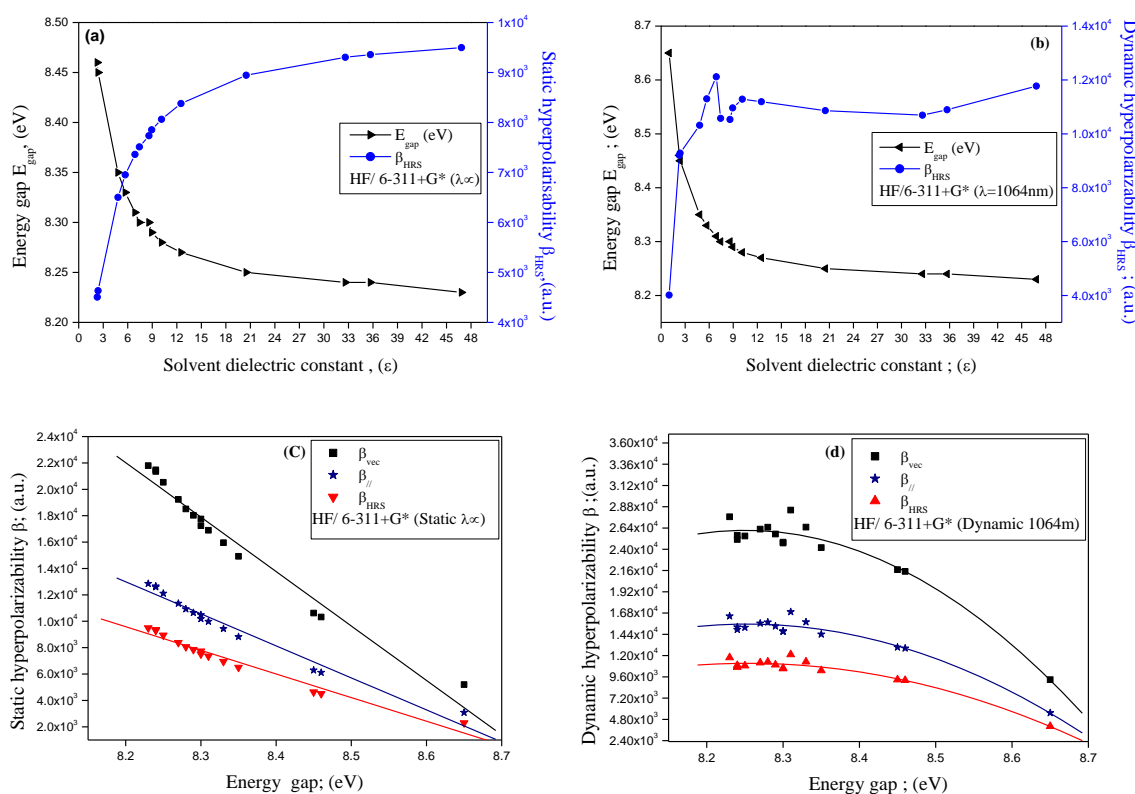


**Fig. 7.** Variation of  $E_{gap}$  and  $\beta_{HRS}$  against solvent dielectric constant ( $\epsilon$ ) (a and b); Relationship between  $E_{gap}$  and first hyperpolarizability  $\beta_{vec}$ ,  $\beta_{//}$  and  $\beta_{HRS}$  (c and d)

When  $E_{gap}$  is plotted against the first hyperpolarizability  $\beta$  with increment in solvent polarity (Fig. 7c and Fig.7d), The best theoretical description of the relationship between the static ( $\lambda=\infty$ ) first hyperpolarizabilities  $\beta_{vec}$ ,  $\beta_{//}$  and  $\beta_{HRS}$  produces high-quality linear dependence behavior (correlation coefficient  $R= 0.98$ ), suggesting that hyperpolarizabilities can effectively be tuned by controlling the electronic transition energy. While at the frequency dependant ( $\lambda =1064nm$ ), the most excellent fits appear to grow within second order polynomial functions (correlation coefficient  $R= 0.97$ ). The best linear and 2<sup>nd</sup> Order polynomial fitting expressions obtained for static ( $\lambda=\infty$ ) and dynamic ( $\lambda= 1064nm$ ) first hyperpolarizabilities ( $\beta_{vec}$ ,  $\beta_{//}$  and  $\beta_{HRS}$ ) as a function of the  $E_{gap}$  are presented as:

For the static ( $\lambda=\infty$ )

Linear equations

$$\beta_{HRS} = 156475.77 - 17913.11 \times (E_{gap}) \quad ; \quad (R = -0.98)$$

$$\beta_{vec} = 360389.87 - 41264.47905 \times (E_{gap}) \quad ; \quad (R = -0.98)$$

$$\beta_{//} = 212058.88054 - 24276.48 \times (E_{\text{gap}}); \quad (R = -0.98)$$

For the dynamic ( $\lambda=1064\text{nm}$ )

2<sup>nd</sup> Order polynomial equations

$$\beta_{\text{HRS}} = -3.08 \times 10^6 + 748846.78 \times (E_{\text{gap}}) - 45366.16 \times (E_{\text{gap}})^2 \quad ; \quad (R = 0.97)$$

$$\beta_{\text{vec}} = -7.19 \times 10^6 + 1.75 \times 10^6 \times (E_{\text{gap}}) - 106018.36 \times (E_{\text{gap}})^2 \quad ; \quad (R = 0.97)$$

$$\beta_{//} = -4.33 \times 10^6 + 1.05 \times 10^6 \times (E_{\text{gap}}) - 63734.85 \times (E_{\text{gap}})^2 \quad ; \quad (R = 0.97)$$

### 3.3.3. The solvent effect on BLA

The solvent effect on geometric structure can also be characterized by the degree of geometric distortion induced by the solvent and defined as the bond length alternation (BLA). A plot of the bond lengths alternation (BLA) as a function of the solvent dielectric constant ( $\epsilon$ ) in parallel with the dipole moment is displayed in Fig. 8. It can be seen that changes in BLA values are generally correlated with the polarity of the solvent. With increasing the solvent dielectric constant, as shown in Fig. 8, the trans  $\alpha,\omega$ -nitro, dimethylamino-hexatriene structures become more distorted as indicated by the decreased BLA values. When passing from benzene  $\epsilon = 2.27$  to acetonitrile  $\epsilon = 35.69$ , the BLA change by  $\approx 0.003 \text{ \AA}$ . However, passing from gas  $\epsilon = 1$  to acetonitrile, the selected BLA change maximally by  $0.036 \text{ \AA}$ . The BLA variation is also accompanied by an important increment in the ground-state dipole moment  $\mu$  ranging from  $12.17 \text{ D}$  for the gas phase to  $16.04 \text{ D}$  for DMSO.

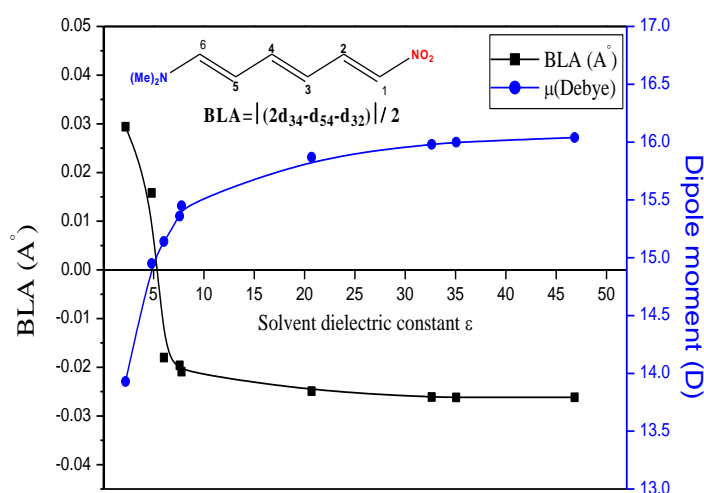


**Fig. 8.** Solvent dependence on BLA and  $\mu$  for all trans  $\alpha,\omega$ -nitro, dimethylamino-Hexatriene

The dipole moment ( $\mu$ ) of all-trans  $\alpha,\omega$ -nitro, dimethylamino-hexatriene is also affected by the solvent polarity. The dipole moment ( $\mu$ ) first increase in the region of  $\epsilon = 1-12.17$  and then gradually come to saturation in the region of  $\epsilon = 13-47$  with an average limiting value of  $\mu = 16$  D. The solvent polarity has a significant impact as the solvent dielectric constant ( $\epsilon$ ) increases.

#### 4. CONCLUSIONS

The second-order nonlinear optical (NLO) properties of a series of substituted hexatriene is revealed on the basis of CPHF and TDHF levels of approximation to assess the effects of bridge length, of frequency dispersion, of the solvent within the polarizable continuum model, of the strength of substituted electron donor groups as well as to establish correlation allowing an easy determination of the first hyperpolarizability  $\beta_{\text{HRS}}$ . Our calculations allow us to identify the main observations are: i) The calculations indicate that the size and solvent effects are combined together to determine the Hyper-Rayleigh scattering response. In particular, the limit when expanding the conjugated system employed to improve the  $\beta_{\text{HRS}}$  has been clearly revealed; ii) The solvent enhances the first hyperpolarizabilities ( $\beta_{\text{HRS}}$ ) significantly by amplitude depending on the polarity of the solvent and the strength of the substituted groups; iii) The specific behavior of the HRS first hyperpolarizability with its anisotropy factor and depolarization ratio as a function of the incident light frequency. However, the solvent effects on anisotropy parameter and depolarization ratio are negligible; iv) A quantitative relationship was established between the first hyperpolarizability  $\beta_{\text{HRS}}$  and the separation distance  $d_{\text{N...N}}$ , energy gap ( $E_{\text{gap}}$ ) and the Kirkwood–Onsager factor  $[(\epsilon - 1) / (2\epsilon + 1)]$ , allowing an easy determination for this quantity.

#### 5. ACKNOWLEDGEMENTS

The author would like to thank Professor Benoit Champagne from Namur University -Belgium for his help (Laboratoire de chimie theorique appliquee. Unité de recherche en chimie physique, théorique et structurale. LCTA-Namur).

## 6. REFERENCES

- [1] Clays.K and André.P. Handbook of advanced electronic and photonic materials and devices. H.S. Nalwa (Eds.), Hyper-rayleigh scattering: Opportunities for molecular, supramolecular, and device characterization by incoherent second-order nonlinear light scattering. San Diego: Academic Press, 2001, pp. 229-266.
- [2] Stegeman G.I, Stegeman R.A. Nonlinear Optics: Phenomena Materials and Devices. New York: Wiley, 2012, pp.15–39.
- [3] Chen K.J, Laurent A.D, Jacquemin D. Strategies for Designing Diarylethenes as Efficient Nonlinear Optical Switches. *J Phys. Chem C.*, 2014, 118(8), 4334– 4345.
- [4] Liu Y, Yuan Y, Tian X, Yuan J, Sun J. Computational design of p-(dimethylamino) benzylidene-derived push-pull polyenes with high first-hyperpolarizabilities. *Phys. Chem. Chem. Phys.*, 2020, 22, 5090–5104.
- [5] Oviedo M.B, Ilawe N.V, Wong B.M. Polarizabilities of  $\pi$ -conjugated chains revisited: improved results from broken-symmetry range-separated DFT and New CCSD(T) benchmarks. *J. Chem. Theory Comput.*, 2016,12(8), 3593–3602.
- [6] Liu Y, Yuan Y, Tian X, Yuan J, Sun J. High first-hyperpolarizabilities of thiobar bituric acid derivative-based donor- $\pi$ -acceptor nonlinear optical-phores: Multiple theoretical investigations of substituents and conjugated bridges effect. *Int. J. Quantum. Chem.*, 2020, e26176, 1–13.
- [7] Meier de Andrade A, Loren Inacio P, Alexandre Camilo Jr. Theoretical investigation of second hyperpolarizability of trans-polyacetylene : Comparison between experimental and theoretical results for small oligomers. *J. Chem. Phys.*, 2015,143, 244906 –7.
- [8] Beverina L, Pagani G.A.  $\Pi$ -Conjugated zwitterions as paradigm of donor acceptor building blocks in organic-based materials. *Acc. Chem. Res.*, 2014, 47(2), 319–329.
- [9] Yanling S, Guochun Y. Non-planar donor–acceptor chiral molecules with large second-order optical nonlinearities: 1,1,4,4-Tetracyanobuta-1,3-diene derivatives. *J. Phys. Chem A*; 2014, 118(6), 1094–1102.
- [10] Hrobarik P, Sigmundova I, Zahradnik P, Kasak P, Arion V, Franz E, Clays K. Molecular



engineering of benzothiazolium salts with large quadratic hyperpolarizabilities. *J Phys.Chem C.*, 2010, 114(50), 22289–22302.

[11] Gorman C.B, Marder S.R. Effect of molecular polarization on bond-length alternation, linear polarizability, first and second hyperpolarizability in donor-acceptor polyenes as a function of chain length. *Chem. Mater.*, 1995, 7(1), 215–220.

[12] Labidi N.S. Semi empirical and Ab initio methods for calculation of polarizability ( $\alpha$ ) and the hyperpolarizability ( $\beta$ ) of substituted polyacetylene chain. *Arabian. J. Chem.*, 2016, 9, 1252–1259.

[13] Tomasi J, Mennucci B, Ammi R. Quantum mechanical continuum solvation models. *Chem. Rev.*, 2005, 105(8), 2999–3094.

[14] Sekino H, Bartlett R. J. Frequency dependent nonlinear optical properties of molecules. *J. Chem. Phys.*, 1986,85(2), 976–989.

[15] Van Gisbergen S.J.A, Snijders J.G, Baerends E.J. Accurate density functional calculations on frequency-dependent hyperpolarizabilities of small molecules. *J. Chem. Phys.*, 1998,109(24), 10657–10668.

[16] Bogdan E, Plaquet A, Antonov L, Rodriguez V, Ducasse L, Champagne B, Castet F. Solvent effects on the second-order nonlinear optical responses in the keto-enol equilibrium of a 2-hydroxy-1-naphthaldehyde derivative. *J. Phys. Chem C.*, 2010, 114(29), 12760–12768.

[17] Yang M, Champagne B. Large off-diagonal contribution to the second-order optical nonlinearities of  $\Lambda$ -shaped molecules. *J. Phys. Chem A.*, 2003, 107(19), 3942–3951.

[18] Jacquemin D, Champagne B, Hättig C. Correlated frequency-dependent electronic first hyperpolarizability of small push–pull conjugated chains. *Chem. Phys. Lett.*, 2000,319(3), 327–334.

[19] Gaussian 09, Revision C. 01, Frisch M.J, Trucks G.W, Schlegel H.B, Scuseria G.E, Robb M.A, Cheeseman JR, Scalmani G, Barone V, Mennucci B, Petersson G.A, Nakatsuji H, Caricato M, Li X, Hratchian H.P, Izmaylov A.F, Bloino J, Zheng G, Sonnenberg J.L, Hada M, Ehara M, Toyota K, Fukuda R, Hasegawa J, Montgomery J.A.J, Peralta J.E, Ogliaro F, Bearpark M, Heyd J.J, Brothers E, Kudin K.N, Staroverov V.N, Kobayashi R, Normand J, Raghavachari K, Rendell A, Burant J.C, Iyengar S, Tomasi J, Cossi M, Rega N, Millam J.M,

---

Klene M, Knox J.E, Cross J.B, Bakken V, Adamo C, Jaramillo J, Gomperts R, Stratmann R.E, Yazyev O, Austin AJ, Cammi R, Pomelli C, Ochterski J.W, Martin R.L, Morokuma K, Zakrzewski V.G, Voth G.A, Salvador P, Dannenberg J.J, Dapprich S, Daniels A.D, Farkas O, Foresman J.B, Ortiz J.V, Cioslowski J, Fox D.J. Gaussian, Inc. Wallingford CT: 2010.

[20] Haynes W.M, Lide D.R, Bruno T.J. CRC Handbook of Chemistry and Physics. 97th Edition. CRC-Press, Boca Raton, 2017. pp.6-199–219.

[21] Woodford J.N, Pauley M.A, Wang C.H. Solvent dependence of the first molecular hyper polarizability of p-nitroaniline revisited. *J. Phys. Chem A.*, 1997, 101(11), 1989–1992.

**How to cite this article:**

Labidi NS. solvent effect on hyper-rayleigh scattering (hrs) first hyperpolarizability of substituted polyene: part (I). *J. Fundam. Appl. Sci.*, 2021, 13(3), 1175-1192.